Facilitation of neural responses to targets moving in three-dimensional optic flow

Sarah Nicholas[1] *and Karin Nordström*[1,2*]

[1]*Flinders Health and Medical Research Institute, Flinders University, GPO Box 2100, Adelaide, SA, 5001, Australia*

[2]*Department of Neuroscience, Uppsala University, Box 593, 751 24 Uppsala, Sweden*

*email: karin.nordstrom@flinders.edu.au

ORCIDs

Sarah Nicholas: 0000-0002-5555-9421

Karin Nordström: 0000-0002-6020-6348

Classification

Biological sciences: Neuroscience

Keywords

Target motion, insect vision, motion vision, background motion, hoverfly, TSDN, wide-field motion, inhibition, facilitation

Abstract

For the human observer, it can be difficult to follow the motion of small objects, especially when they move against background clutter. However, insects efficiently do this, as evidenced by their ability to capture prey, pursue conspecifics, or defend territories, even in highly textured surrounds. This behavior has been attributed to optic lobe neurons that are sharply tuned to the motion of small targets, as these neurons respond robustly even to a target moving against background motion. However, the target selective descending neurons (TSDNs), that more directly control behavioral output, do not. Importantly, though, the backgrounds used previously not only lacked 3D motion cues, but also high-contrast features, both of which would be encountered during natural behaviors. To redress this deficiency, we here use backgrounds consisting of many targets moving coherently to simulate the type of 3D optic flow that would be generated by an insect's own motion through the world. We show that hoverfly TSDNs do not respond to this type of optic flow, even though it contains features with spatio-temporal profiles similar to optimal targets. However, TSDN responses are inhibited when this optic flow is shown together with a target. More surprisingly, TSDNs are facilitated by horizontal, frontal optic flow in the opposite direction to target motion. We show that these interactions are likely inherited from the pre-synaptic neurons, and argue that the facilitation could benefit the initiation of target pursuit.

Significance statement

Target detection in visual clutter is a difficult computational task that insects, with their poor resolution compound eyes and small brains, do successfully and with extremely short behavioral delays. We here show that target neurons do not respond to widefield motion consisting of a multitude of "targets", suggesting that the hoverfly visual system interprets coherent widefield motion differently from the motion of individual targets. In addition, we show that widefield motion in the opposite direction to target motion increases the neural response. This is an incredibly non-intuitive finding, and difficult to reconcile with current models for target selectivity, but has behavioral relevance.

47 **/body**

48 ## Introduction

49 The survival of many animals often depends on their ability to visually detect small moving
50 objects or targets, as these could represent predators, prey, mates or territorial intruders
51 (1). Efficient target detection is a computationally challenging task, which becomes even
52 more difficult when done against visual clutter. Despite this, many insects successfully
53 detect targets, followed by highly acrobatic pursuits, often in visually complex
54 environments. For example, male *Eristalis tenax* hoverflies establish territories in foliage rich
55 areas, on alert for intruders and ready to engage in high-speed pursuit (2).

56 Initial target detection can be facilitated by behaviors that render the background
57 stationary, thus making the target the only thing that moves. Many insects and vertebrates
58 thus visualize targets against the bright sky (3), or from a stationary stance, such as perching
59 (4-6) or hovering (7, 8). However, as soon as the pursuer moves, this creates self-generated
60 optic flow (9), against which the independent motion of the target needs to be
61 discriminated. That insects do this successfully is remarkable considering their small brains
62 and low-resolution compound eyes (10), suggesting a high level of optimization.

63 Predatory dragonflies and territorial hoverflies, which both pursue targets, have sharply
64 tuned small target motion detector (STMD) neurons in their optic lobes (11, 12).
65 Impressively, some STMDs respond robustly to targets in clutter, even without relative
66 velocity differences (12, 13), suggesting that they could support behavioral pursuit against
67 self-generated optic flow. However, the target selective descending neurons (TSDNs), which
68 are thought to be post-synaptic to STMDs (14), do not respond to targets moving across syn-

69 directional background motion (15). This is peculiar as descending neurons more directly
70 drive behavioral output (16, 17). Importantly, however, the backgrounds used in previous
71 STMD (12, 13, 18) and TSDN (15) experiments consisted of panoramic images that were
72 displaced across the visual monitor, lacking the 3D cues associated with real pursuits (19,
73 20). In addition, even if some backgrounds had spatial statistics resembling natural images
74 (21) they lacked the high-contrast edges often found in natural scenes. Where naturalistic
75 backgrounds contained small, high-contrast features, these would often generate STMD
76 responses (13). Indeed, it is highly likely that STMDs generate their ability to detect targets
77 in clutter by being sharply tuned to the target's unique spatio-temporal profile (22).

78 To investigate TSDN responses to targets in background motion, under more dynamic
79 conditions, we used an optic flow stimulus consisting of many "targets" simulated to move
80 coherently around the fly's point of view (23). We use this to simulate the type of optic flow
81 generated during translations and rotations through the world. Importantly, the individual
82 components that make up the optic flow contain the same high-contrast edges as the target
83 itself, against which target motion can only be determined by its independent trajectory.
84 We quantified the responses of *Eristalis* TSDNs to targets moving against 6 types of optic
85 flow (23), three translations and three rotations. We found that optic flow on its own did
86 not generate any TSDN response, even when moving in the neuron's preferred direction,
87 and despite it consisting of many "targets". Consistent with previous results (15), we found
88 that optic flow in the same direction as the target inhibits the TSDN response. Importantly,
89 inhibition occurred even if the optic flow only preceded target motion and did not appear
90 concurrently. Most strikingly we showed that optic flow in the opposite direction to target

91 motion increased the TSDN response. This facilitation required opposing horizontal optic
92 flow in the frontal visual field. Such neural facilitation is a novel observation.

93 ## Results

94 ### *3D optic flow strongly affects the TSDN response to target motion*

95 We recorded extracellularly from target selective descending neurons (TSDNs) in male
96 *Eristalis tenax* hoverflies. TSDNs respond strongly to the motion of a small, dark target (15,
97 23), traversing a white background (Fig. 1A, B, Movie 1, 2, Fig. S1A-C). We used a 3D optic
98 flow stimulus simulating the coherent motion of many "targets" (23) around the hoverfly's
99 position. Against this optic flow, representing retinal flow fields experienced during flight
100 through the world, the target can only be identified by its independent trajectory. Indeed,
101 when both are stationary, there are no features identifying the target (Fig. 1A). Despite this,
102 TSDNs respond strongly to targets moving across stationary optic flow (Fig. 1B; Movie 3, 4;
103 Fig. S1A-C).

104 For quantification, we calculated the mean spike frequency for the duration of target
105 motion, after excluding the first and last 40 ms (dotted box, Fig. S1A-C). We found a small,
106 significant response reduction to targets moving across stationary optic flow compared with
107 a white background (Fig. 1B). As the response across neurons was variable (N=34,
108 coefficient of variation 60% and 63%, respectively, Fig. 1B), we normalized the response
109 from each neuron to its own mean response to a target moving across a white background.

110 We found that when the target moved horizontally across sideslip optic flow moving in the
111 same direction, the TSDN response was strongly inhibited (Fig. 1C, D, "Sideslip +50"),

compared with control where the target moved over stationary optic flow (grey, Fig. 1C, D). Yaw optic flow in the same direction as the target also strongly inhibited the TSDN response (Fig. 1C, D, "Yaw +50"). This complete inhibition is striking (Movie 5, 6), but consistent with previous TSDN work using sliding background images (15).

In contrast, when the sideslip moved in the opposite direction to the target the TSDN response was strongly enhanced (Movie 7, 8, Fig. 1C, D, "Sideslip -50", mean increase 71.1%). Similarly, yaw optic flow in the opposite direction to the target also facilitated the TSDN response, by 84.9% (Fig. 1C, D, "Yaw -50"). Such response facilitation was not seen when displaying targets moving over panoramic background images, in either TSDNs (15) or other target tuned neurons in the fly optic lobes (12, 18, 24).

At any one time the optic flow itself contained ca. 1200 "targets" moving coherently on the display in front of the fly (23). When the sideslip moved in the TSDN's preferred direction tens of these "optic flow targets" moved through the TSDN receptive field (Movie 5, 6). Despite this, preferred direction sideslip without target motion only generated a response in 18% of 222 repetitions across 12 TSDNs (Fig. S1D, "Sideslip +50"). In addition, when preferred direction sideslip did generate a TSDN response, this was less than one-fifth of the response to a target traversing a white background (Fig. S1E, "Sideslip +50"). This suggests that the coherent motion of the "targets" in the optic flow is treated differently from the motion of a single target.

We next investigated the effect other types of 3D optic flow had on TSDN responses to target motion. We found that the target response was inhibited by lift (mean 44.0% response for downwards lift, "Lift +50"; mean 34.3% for upwards lift, "Lift -50", Fig. S2).

When the target was displayed against pitch, which provides similar vertical motion in the frontal visual field, the response was suppressed to similar levels (57.1%, "Pitch +50"; 54.9%, "Pitch -50", Fig. S2). In addition, the target response was inhibited to roughly similar levels when displayed against thrust or roll optic flow in either direction (Fig. S2). No optic flow generated a substantial TSDN response when displayed on its own (Fig. S1D, E).

Inherited optic flow interactions

Our data show that optic flow significantly affects the TSDN response to target motion (Fig. 1, S2). Where does the optic flow pathway interact with the target motion pathway? If widefield sensitive neurons interact directly with the TSDNs, as previously suggested (15), the optic flow should act independently. That is, if the target changes direction but the optic flow remains the same, the influence the optic flow has on the TSDN response should remain similar. In contrast, if the interaction is inherited from pre-synaptic neurons, we expect the TSDN response to show significant interaction between target direction and optic flow direction.

We investigated this by recording from TSDNs that respond robustly both to horizontal (grey, Fig. S3) and vertical target motion (black, Fig. S3), displayed against either sideslip or lift (Fig. 2). As above (Fig. 1, S2), the TSDN response was inhibited when a horizontally moving target was displayed against sideslip or lift (Fig. 2A). If the target instead moved vertically against sideslip or lift, a two-way ANOVA showed that neither the target direction nor the optic flow direction had a significant effect on the TSDN response (Fig. 2A). However, there was a significant interaction between target direction and optic flow

direction (P=0.0002, two-way ANOVA), consistent with the hypothesis that the interaction is inherited from the pre-synaptic neurons.

As above (Fig. 1, S2), the TSDN response was facilitated when a target moved horizontally against sideslip in the opposite direction, but inhibited against lift (Fig. 2B). When comparing this to vertical target motion, a two-way ANOVA showed that both the target direction and the optic flow direction significantly affected the TSDN response (Fig. 2B, P=0.0092 and P=0.0228, respectively). In addition, there was a significant interaction between target direction and optic flow direction (P=0.0010, two-way ANOVA, Fig. 2B), consistent with the hypothesis that the interaction is inherited from pre-synaptic neurons.

Presynaptic neurons

From which pre-synaptic neurons do the TSDNs inherit these interactions? TSDNs have been proposed to get their input from STMDs (25), but this has never been shown conclusively, and in addition, there are many other target tuned neurons in the fly optic lobes (e.g. 24, 26-29). We can investigate this by looking at the underlying target tuning mechanisms, which can be distilled down into three fundamentally different concepts. For example, visual neurons can become target tuned by receiving inhibitory feedback from the widefield system (29-31), or by using center-surround antagonism together with rapid adaptation (28, 32). Alternatively, they can use an elementary STMD model, which is tuned to the unique spatio-temporal profile of a moving target, with a dark contrast change (OFF) from the leading edge followed by a bright contrast change (ON) by the trailing edge. Importantly, while the first two mechanisms rely on comparisons from neighboring points in space, the elementary STMD compares input from one point on space (22, 28, 33). Therefore, the first

two models will respond equally well to the motion of a target, to the motion of a leading OFF edge, and the motion of a trailing ON edge (black, Fig. 3, redrawn from (28, 34)). In contrast, the elementary STMD model only responds strongly to the target (grey, Fig. 3, redrawn from (34)).

Our results show that TSDNs do not respond well to a leading OFF edge, or to a trailing ON edge (white, Fig. 3). However, a complete target, where the leading edge is rapidly followed by a trailing edge, gives a robust TSDN response (white, Fig. 3). Indeed, the physiological responses (white, Fig. 3) match the elementary STMD model output (grey, Fig. 3). Since STMD physiology also matches the elementary STMD model output (13, 34), this suggests that TSDNs receive input from STMDs.

TSDN responses are inhibited by preceding optic flow

In dragonflies, STMD target responses can be primed by preceding target motion, thereby facilitating responses to longer target trajectories (35, 36). To investigate if the optic flow can similarly prime TSDN responses, we displayed preceding optic flow for 1 s (green, Fig. 4A), followed by optic flow concurrent (red, Fig. 4A) with target motion (blue, Fig. 4A). We found that when the sideslip moved in the same direction as the target, both the preceding and concurrent optic flow had a significant effect on the TSDN response (2-way ANOVA, $P=0.0032$ for preceding optic flow and $P=0.0003$ for concurrent optic flow). A Bonferroni multiple comparison's test showed that the preceding optic flow had a significant effect when the optic flow was stationary concurrent with target motion (Fig. 4B), but not when it was moving (Fig. 4C).

198 In the inverse experiment, when the sideslip moved in the opposite direction to the target,
199 only the concurrent optic flow had a significant effect on the TSDN response (2-way ANOVA,
200 P=0.58 for preceding, and P=0.0056 for concurrent optic flow). Thus, preceding sideslip in
201 the opposite direction to target motion did not facilitate the TSDN response (Fig. 4D).
202 Neither did the facilitation depend on whether the optic flow was in motion or stationary
203 prior to target motion (Fig. 4E).

204 ***Frontal optic flow is essential***

205 Our results show that yaw and sideslip optic flow have similar effects on TSDN target
206 responses (Fig. 1). As both sideslip and yaw contain substantial motion in the frontal visual
207 field (37), we next asked if frontal optic flow is required. We investigated this by limiting the
208 spatial extent of sideslip to either cover the ipsilateral, dorsal, ventral or contralateral
209 position on the screen (Fig. 5A). Note that only the dorsal position covers the TSDN
210 receptive field (Fig. 5A). In the other three positions, the sideslip was spatially separated
211 from the receptive field (Fig. 5A).

212 We found that when sideslip moved in the same direction as the target, the TSDN response
213 was inhibited if the optic flow covered the full, dorsal or ventral position on the screen (Fig.
214 5B), compared with the stationary control (grey, Fig. 5B). However, when optic flow only
215 covered the ipsilateral or contralateral positions, there was no inhibition (Fig. 5B),
216 suggesting that frontal optic flow is required. Our results are consistent with inhibition
217 driven by panoramic background images, which do not have to spatially overlap the target
218 trajectory, or have a large spatial extent (15).

We found that when sideslip moved in the opposite direction to the target, the TSDN response was facilitated if the optic flow covered the full, dorsal or ventral positions on the screen (Fig. 5C). When the optic flow was limited to the ipsilateral or contralateral positions, there was no facilitation (Fig. 5C). This suggests that the optic flow does not have to spatially overlap with the TSDN receptive field. However, there has to be frontal opposite direction sideslip for facilitation to take place.

Discussion

We generated optic flow using the coherent motion of thousands of "targets" within a simulated 3D space (23) and recorded from TSDNs, which respond to the motion of small targets (Fig. 1). We found that even when the "targets" in the optic flow moved in the neuron's preferred direction, there was no response (Fig. S1D, E). However, when the optic flow was displayed together with a target, this modulated the TSDN's target response (Fig. 1, S2). In particular, optic flow in the opposite direction to target motion strongly enhanced the TSDN response, whereas optic flow in the same direction inhibited the response (Fig. 1).

The effect optic flow has on the TSDN response to target motion (Fig. 1, S2) could be inherited from the neurons that are pre-synaptic to the TSDNs, or alternatively, TSDNs could receive input from widefield motion sensitive neurons, as previously suggested (15). However, we found e.g. that while the response to a target moving horizontally across syn-directional sideslip was strongly inhibited, if the target moved vertically against the same sideslip, the TSDN response was much larger (Fig. 2A). This argues against direct input from the widefield motion vision pathway, as we would expect the same optic flow to have the same effect on the TSDN response, irrespective of target direction. Instead, we found

241 significant interactions between target direction and optic flow direction (Fig. 2), making it
242 likely this is inherited from the pre-synaptic neurons.

243 What are the pre-synaptic candidates? Even if TSDNs have been suggested to get input from
244 STMDs (25), there are other optic lobe neurons tuned to the motion of targets, also referred
245 to as objects, or figures (24, 26-29). For example, blowfly lobula plate figure detection (FD)
246 cells receive inhibitory input from widefield motion sensitive neurons (38), thereby making
247 them respond to the independent motion of a figure (29-31). However, FD cells are not as
248 sharply tuned to small targets (33) as TSDNs (15), and they are inhibited by background
249 motion in the same and in the opposite direction (29), unlike our findings (Fig. 1C, D),
250 making it unlikely that they provide the TSDN input.

251 Another option are the anatomically defined *Drosophila* lobula columnar (LC) neurons (39).
252 Whereas some LC neurons respond better to bars or widefield motion, LC11 and LC26
253 neurons respond strongly to small targets (24, 40). Besides being sharply size-tuned, LC11
254 neurons are clearly involved in behavioral responses to small objects (27, 28). LC11 small
255 object selectivity can be explained using a combination of center-surround antagonism and
256 rapid adaptation (28), making them inhibited by background motion in either direction (26),
257 inconsistent with our TSDN facilitation (Fig. 1C, D). Potentially, facilitation could be achieved
258 by making the influence of the surround directional (32). However, as the optic flow did not
259 have to cover the TSDN receptive field to have an effect ("ventral", Fig. 5), such center-
260 surround mechanisms are unlikely.

261 Importantly, as both FD cells and LC11 neurons rely on an input from at least two points in
262 space (28, 33), they respond to high-contrast changes associated with sweeping edges (28,

34), as well as to complete targets (black, Fig. 3). In contrast, TSDNs respond much better to a complete target, than to either OFF or ON contrast changes (white, Fig. 5), i.e. consistent with input from elementary STMDs (22). Since the elementary STMD model provides robust predictions of physiological STMD responses in dragonflies (13, 34), we conclude that it is likely that TSDNs get their input from STMDs.

At a first glance, this seems counterintuitive, as some STMDs respond robustly to targets in background motion, even without relative motion cues (12), whereas we saw inhibition to targets displayed against syn-directional optic flow (Fig. 1C, D). In addition, the elementary STMD model predicts that target-like features in the background should generate a response (22). In our TSDN experiments, despite the optic flow consisting of "targets" with optimal spatio-temporal profiles (Movie 5, 6), there were no consistent responses to preferred direction optic flow (e.g. "Sideslip +50", "Yaw +50", Fig. S1D, E, see also raw data, Fig. 4A).

However, STMDs are a heterogeneous group (12), and in some STMDs responses to target motion are decreased by syn-directional background motion (18). Indeed, the centrifugal STMDs that respond most robustly to targets against background motion (12, 13), and that respond to background features with target-like profiles (13), do not project to pre-motor areas, but contralaterally through the protocerebrum, with outputs in the heterolateral lobula (12, 41). This suggests a role in modulating the responses of other optic lobe neurons, rather than providing direct input to descending neurons (14). In contrast, the STMDs that have small receptive fields, and outputs in pre-motor areas of the lateral mid-brain, and that are therefore more likely to be pre-synaptic to the TSDNs, are often inhibited by background motion (18).

Our data suggest that inhibition and facilitation are not necessarily generated by the same mechanism. For example, most types of optic flow generated inhibition (Fig. S2), but only opposite direction yaw and sideslip led to facilitation (Fig. 1C, D). In addition, unlike facilitation, inhibition could be primed (Fig. 4). Importantly, the facilitation of TSDN responses to target motion displayed on optic flow in the opposite direction (Fig. 1C, D) is a novel observation. In previous work using panoramic background images, TSDN responses were significantly reduced when the background moved in the opposite direction to the target (15). This suggests that facilitation is not generated by a widefield motion sensitive neuron, as such a neuron would respond to panoramic background images (15) as well as to optic flow (23).

The elementary STMD model predicts a response to the "targets" in the optic flow (22), as these have correct spatio-temporal profiles. While the TSDN response matches the elementary STMD model (Fig. 3), TSDNs do not respond to optic flow when displayed alone (Fig. S1D, E), therefore suggesting pre-synaptic inhibition from the widefield motion pathway (Fig. 2). However, STMDs with input from elementary STMDs, but without inhibition from widefield motion, should respond to the "targets" in optic flow, as evidenced by dragonfly centrifugal STMDs (13). In contrast, background images lacking high-contrast features do not generate a response in centrifugal STMDs (12, 13). Therefore, such STMDs may drive the TSDN facilitation. Given facilitation requires frontal, horizontal motion (Fig. 5), these neurons would likely have frontal receptive fields. The centrifugal STMDs have large receptive fields (12, 41), suggesting that ipsilateral or contralateral optic flow should also drive facilitation, which it did not (Fig. 5). Importantly, however, there are at least 20

different STMD types in the hoverfly lobula (12), suggesting that future investigation of STMD responses to targets in clutter are required to identify the neurons driving facilitation.

Nevertheless, the facilitation could make behavioral sense. Prior to initiating target pursuit, male *Eristalis* hoverflies have been described to predict the flight course required to successfully intercept the target, based predominantly on the target's angular velocity (42). To successfully execute an interception style flight course, the hoverfly turns in the direction that the target is moving (42). In doing so, the hoverfly creates self-generated optic flow in the opposite direction to the target's motion. If the TSDNs that we have recorded from here are involved in such planning of pursuit, they would be facilitated when the target moves in the opposite direction to the self-generated optic flow (Fig. 1C, D), which might be beneficial for controlling behavioral output. Reconstructing retinal flow fields as experienced during actual pursuits (19) could help address this question.

Materials and Methods

Electrophysiology

Eristalis tenax hoverflies were reared and maintained as previously described (43). For electrophysiology, a male hoverfly was immobilized ventral side up using a beeswax and resin mixture. A small hole was cut at the anterior end of the thorax to expose the cervical connective, which was then raised slightly and supported using a small wire hook, for insertion of a sharp polyimide-insulated tungsten microelectrode (2 MOhm, Microprobes, Gaithersburg, USA). The animal was grounded via a silver wire inserted into the ventral part of the hole.

329 Extracellular signals were amplified at 100x gain and filtered through a 10- to 3000-Hz
330 bandwidth filter on a DAM50 differential amplifier (World Precision Instruments, Sarasota,
331 USA), with 50 Hz noise removed with a HumBug (Quest Scientific, North Vancouver,
332 Canada). The data were digitized via Powerlab 4/30 (ADInstruments, Sydney, Australia) and
333 acquired at 40 kHz with LabChart 7 Pro software (ADInstruments). Single units were
334 discriminated by amplitude and half-width using Spike Histogram software (ADInstruments).

335 ***Visual stimuli***

336 *Eristalis* males were placed ventral side up, centered and perpendicular to an Asus LCD
337 screen (Asus, Taipai, Taiwan) at 6.5 cm distance. The screen had a refresh rate of 165 Hz, a
338 linearized contrast with a mean illuminance of 200 Lux, and a spatial resolution of 2560 x
339 1440 pixels, giving a projected screen size of 155° x 138°. Visual stimuli were displayed using
340 custom written software based on the Psychophysics toolbox (44, 45) in Matlab
341 (Mathworks, Natick, USA).

342 TSDNs were identified as described (15, 23). In short, we mapped the receptive field of each
343 neuron by scanning a target horizontally and vertically at 20 evenly spaced elevations and
344 azimuths (23), to calculate the local motion sensitivity and local preferred direction. We
345 then scanned targets of varying height through the small, dorso-frontal receptive fields (Fig.
346 4A) to confirm that each neuron was sharply size tuned with a peak response to targets
347 subtending 3°- 6°, with no response to larger bars, to looming or to widefield stimuli (15,
348 23).

349 Unless otherwise mentioned, targets were black and round with a diameter of 15 pixels,
350 moving at a velocity of 900 pixels/s for 0.48 s. When converted to angular values and taking

the small frontal receptive fields of TSDNs into account, this corresponds to an average diameter of 3° and a velocity of 130°/s (15). Unless otherwise stated, each target travelled in each neuron's preferred horizontal direction (i.e. left or right) and across the center of its receptive field. Between repetitions, we varied the target elevation slightly, to minimize habituation (15). There was a minimum 4 s between stimulus presentations. Stimulus order was randomized.

For input mechanism experiment (Fig. 3), targets were black and square with a side of 15 pixels, moving at a velocity of 900 pixels/s. OFF and ON edges had a height of 15 pixels. All stimuli started at the far edge of the screen moving in each neuron's preferred direction, across the entire width of the screen.

3D optic flow was generated as previously described (23). Briefly, the optic flow consisted of a simulated cube with 4 m sides, filled with 2 cm diameter spheres at a density of 100 per m^3, with the hoverfly placed in the center. The coherent motion of these ca 6400 spheres around the hoverfly was used to simulate self-generated optic flow. The ca 1200 spheres anterior to the hoverfly were projected onto the screen, with their size indicating the distance from the hoverfly. Circles closer than 6 cm were not displayed. Six types of optic flow were simulated: three translations at 50 cm/s (sideslip, lift and thrust) and three rotations at 50°/s (yaw, pitch and roll). Unless otherwise stated optic flow was displayed for 0.48 s prior to the target. Both target motion and optic flow disappeared simultaneously.

In most experiments the optic flow covered the entire visual display. In some experiments, we limited the spatial extent of the optic flow, into 4 spatial positions (Fig. 5A). TSDN receptive fields tend to be located slightly offset from the visual midline, with preferred

373 direction of motion away from the midline (Fig. 5A). We defined the lateral parts of the
374 display as either ipsilateral or contralateral based on the preferred direction of each TSDN.

375 ***Data analysis and statistics***

376 We recorded from 34 TSDNs in 34 male hoverflies. We kept data from all TSDNs that
377 showed a robust response to a target moving over a white background (Fig. 1B, Movie 1, 2).
378 We repeated this control throughout the recording, and only kept data from neurons that
379 responded consistently. We only kept data from experiments with a minimum 9 repetitions.
380 The data from repetitions within a neuron were averaged, and shown as spike histograms
381 (mean ± sem) with 1 ms resolution, after smoothing with a 20 ms square-wave filter. For
382 quantification across neurons in most cases, we calculated the mean spike rate for each
383 neuron from the spike histogram for the duration of target motion, after excluding the first
384 and last 40 ms (dotted boxes, Fig. S1B-E). We normalized the responses to each neuron's
385 own mean response to a target moving over a white background.

386 For the model experiment (Fig. 3), we calculated the mean spike rate across 0.48 s from the
387 spike histogram when the target traversed each neuron's receptive field. We normalized
388 the data from each neuron to the sum of the responses to the three stimuli (ON, OFF,
389 target).

390 Data analysis was performed in Matlab and statistical analysis in Prism 7.0c for Mac OS X
391 (GraphPad Software, San Diego, USA). Throughout the paper *n* refers to the number of
392 repetitions within one neuron, and *N* to the number of neurons. The sample size, type of
393 test and P value is indicated in each figure legend. We performed paired t-tests, one-way
394 ANOVAs, followed by Dunnett's post hoc test for multiple comparisons, or two-way RM

395 ANOVAs, followed by Bonferroni's post hoc test for multiple comparisons. All data have
396 been deposited to DataDryad.

397 Acknowledgements

398 We thank lab members for constructive feedback, and the Botanic Gardens of Adelaide for
399 their ongoing support. This research was funded by the US Air Force Office of Scientific
400 Research (AFOSR, FA9550-19-1-0294), the Australian Research Council (ARC, DP170100008,
401 DP180100144 and FT180100289), and the Flinders Foundation.

402

References

1. P. T. Gonzalez-Bellido, S. T. Fabian, K. Nordström, Target detection in insects: optical, neural and behavioral optimizations. *Curr Opin Neurobiol* **41**, 122-128 (2016).
2. W. Wellington, S. Fitzpatrick, Territoriality in the drone fly, *Eristalis tenax* (Diptera, Syrphidae). *Can Entomol* **113**, 695-704 (1981).
3. J. Zeil, Sexual dimorphism in the visual system of flies: The free flight behavior of male Bibionidae (Diptera). *J Comp Physiol A* **150**, 395-412 (1983).
4. S. T. Fabian, M. E. Sumner, T. J. Wardill, S. Rossoni, P. T. Gonzalez-Bellido, Interception by two predatory fly species is explained by a proportional navigation feedback controller. *Journal of The Royal Society Interface* **15** (2018).
5. R. Schröder, C. N. Linkem, J. A. Rivera, M. A. Butler, Should I stay or should I go? Perching damselfly use simple colour and size cues to trigger flight. *Animal Behaviour* **145**, 29-37 (2018).
6. C. T. O'Rourke, T. Pitlik, M. Hoover, E. Fernández-Juricic, Hawk eyes II: diurnal raptors differ in head movement strategies when scanning from perches. *PLoS One* **5**, e12169 (2010).
7. S. M. Fitzpatrick, W. G. Wellington, Contrasts in the territorial behavior of three species of hover flies (Diptera: Syrphidae). *Can Entomol* **115**, 559-566 (1983).
8. E. L. Corvidae, R. O. Bierregaard, S. E. Peters, Comparison of wing morphology in three birds of prey: correlations with differences in flight behavior. *J Morphol* **267**, 612-622 (2006).
9. J. J. Koenderink, Optic flow. *Vision Res* **26**, 161-179 (1986).
10. M. F. Land, Visual acuity in insects. *Annu Rev Entomol* **42**, 147-177 (1997).

11. D. O'Carroll, Feature-detecting neurons in dragonflies. *Nature* **362**, 541-543 (1993).

12. K. Nordström, P. D. Barnett, D. C. O'Carroll, Insect detection of small targets moving in visual clutter. *PLoS Biol* **4**, 378-386 (2006).

13. S. D. Wiederman, D. C. O'Carroll, Discrimination of features in natural scenes by a dragonfly neuron. *J Neurosci* **31**, 7141-7144 (2011).

14. K. Nordström, Neural specializations for small target detection in insects. *Curr Opin Neurobiol* **22**, 272-278 (2012).

15. S. Nicholas, J. Supple, R. Leibbrandt, P. T. Gonzalez-Bellido, K. Nordström, Integration of small- and wide-field visual features in Target-Selective Descending Neurons of both predatory and non-predatory dipterans. *J Neurosci* **38**, 10725-10733 (2018).

16. S. Namiki, M. H. Dickinson, A. M. Wong, W. Korff, G. M. Card, The functional organization of descending sensory-motor pathways in *Drosophila*. *eLife* **7**, e34272 (2018).

17. C. L. Chen *et al.*, Imaging neural activity in the ventral nerve cord of behaving adult *Drosophila*. *Nat Commun* **9**, 4390 (2018).

18. P. D. Barnett, K. Nordström, D. C. O'Carroll, Retinotopic organization of small-field-target-detecting neurons in the insect visual system. *Curr Biol* **17**, 569-578 (2007).

19. T. Wardill *et al.*, A novel interception strategy in a miniature robber fly with extreme visual acuity. *Curr Biol* **27**, 854-859 (2017).

20. R. M. Olberg, A. H. Worthington, J. L. Fox, C. E. Bessette, M. P. Loosemore, Prey size selection and distance estimation in foraging adult dragonflies. *J Comp Physiol A* **191**, 791-797 (2005).

21. O. Dyakova, Y.-J. Lee, K. D. Longden, V. G. Kiselev, K. Nordström, A higher order visual neuron tuned to the spatial amplitude spectra of natural scenes. *Nat Commun* **6**, 8522 (2015).

22. S. D. Wiederman, P. A. Shoemaker, D. C. O'Carroll, A model for the detection of moving targets in visual clutter inspired by insect physiology. *PLoS ONE* **3**, e2784 (2008).

23. S. Nicholas, R. Leibbrandt, K. Nordström, Visual motion sensitivity in descending neurons in the hoverfly. *J Comp Physiol A* **206**, 149-163 (2020).

24. C. Städele, M. F. Keleş, J. M. Mongeau, M. A. Frye, Non-canonical receptive field properties and neuromodulation of Feature-Detecting neurons in flies. *Curr Biol* 10.1016/j.cub.2020.04.069 (2020).

25. K. Nordström, D. C. O'Carroll, Feature detection and the hypercomplex property in insects. *Trends Neurosci* **32**, 383-391 (2009).

26. M. F. Keleş, B. J. Hardcastle, C. Städele, Q. Xiao, M. A. Frye, Inhibitory interactions and columnar inputs to an object motion detector in *Drosophila*. *Cell Rep* **30**, 2115-2124.e2115 (2020).

27. M. F. Keleş, M. A. Frye, Object-detecting neurons in *Drosophila*. *Curr Biol* **27**, 680-687 (2017).

28. R. Tanaka, D. A. Clark, Object-displacement-sensitive visual neurons drive freezing in *Drosophila*. *Curr Biol* 10.1016/j.cub.2020.04.068 (2020).

29. M. Egelhaaf, On the neuronal basis of figure-ground discrimination by relative motion in the visual system of the fly. II. Figure-detection cells, a new class of visual interneurones. *Biol Cybern* **52**, 195-209 (1985).

30. A. K. Warzecha, M. Egelhaaf, A. Borst, Neural circuit tuning fly visual interneurons to motion of small objects. I. Dissection of the circuit by pharmacological and photoinactivation techniques. *J Neurophysiol* **69**, 329-339 (1993).

31. W. Reichardt, T. Poggio, Figure-ground discrimination by relative movement in the visual-system of the fly. Part I: Experimental results. *Biol Cybern* **35**, 81-100 (1979).

32. T. Collett, Visual neurones in the anterior optic tract of the privet hawk moth. *J Comp Physiol* **78**, 396-433 (1972).

33. M. Egelhaaf, On the neuronal basis of figure-ground discrimination by relative motion in the visual system of the fly. III. Possible input circuitries and behavioral significance of the FD-cells. *Biol Cybern* **52**, 267-280 (1985).

34. S. D. Wiederman, P. A. Shoemaker, D. C. O'Carroll, Correlation between OFF and ON Channels Underlies Dark Target Selectivity in an Insect Visual System. *J Neurosci* **33**, 13225-13232 (2013).

35. S. D. Wiederman, J. M. Fabian, J. R. Dunbier, D. C. O'Carroll, A predictive focus of gain modulation encodes target trajectories in insect vision. *eLife* **6** (2017).

36. K. Nordström, D. M. Bolzon, D. C. O'Carroll, Spatial facilitation by a high-performance dragonfly target-detecting neuron. *Biol Lett* **7**, 588-592 (2011).

37. M. O. Franz, H. G. Krapp, Wide-field, motion-sensitive neurons and matched filters for optic flow fields. *Biol Cybern* **83**, 185-197 (2000).

38. A. K. Warzecha, A. Borst, M. Egelhaaf, Photo-ablation of single neurons in the fly visual system reveals neural circuit for the detection of small moving objects. *Neurosci Lett* **141**, 119-122 (1992).

493 39. J. W. Aptekar, M. F. Keles, P. M. Lu, N. M. Zolotova, M. A. Frye, Neurons forming
494 optic glomeruli compute figure-ground discriminations in *Drosophila*. *J Neurosci* **35**,
495 7587-7599 (2015).
496 40. M. Wu *et al.*, Visual projection neurons in the *Drosophila* lobula link feature
497 detection to distinct behavioral programs. *eLife* **5**, e21022 (2016).
498 41. B. R. H. Geurten, K. Nordström, J. D. H. Sprayberry, D. M. Bolzon, D. C. O'Carroll,
499 Neural mechanisms underlying target detection in a dragonfly centrifugal neuron. *J*
500 *Exp Biol* **210**, 3277-3284 (2007).
501 42. T. S. Collett, M. F. Land, How hoverflies compute interception courses. *J Comp*
502 *Physiol A* **125**, 191-204 (1978).
503 43. S. Nicholas, M. Thyselius, M. Holden, K. Nordström, Rearing and long-term
504 maintenance of *Eristalis tenax* hoverflies for research studies. *JoVE*
505 doi:10.3791/57711, e57711 (2018).
506 44. D. H. Brainard, The Psychophysics toolbox. *Spatial Vision* **10**, 433-436 (1997).
507 45. D. G. Pelli, The VideoToolbox software for visual psychophysics: Transforming
508 numbers into movies. *Spatial Vision* **10**, 437-442 (1997).
509

510

Figure Legends

Figure 1. The TSDN response to target motion is affected by horizontal optic flow

A) Pictograms of the round, black target, with a diameter of 3°, traversing a white background (left), or stationary optic flow (right), at 130°/s. **B)** The mean spiking response of different TSDNs was significantly reduced when the target moved across stationary optic flow compared with a white background (N=34; ***P < 0.001, two-tailed paired t-test). **C)** The TSDN response to a target traversing stationary optic flow (left, grey), sideslip or yaw in either the same or the opposite direction to the target (red pictograms). All histograms from a single TSDN (mean ± sem, n=18) shown with 1 ms resolution after smoothing with a 20 ms square-wave filter. **D)** The mean response across TSDNs (N=12) to a target traversing stationary optic flow (left, grey), sideslip or yaw, in the same direction ("+50") or opposite direction ("-50") to the target, after normalizing the data to each neuron's own response to a target traversing a white background. Sideslip was simulated at 50 cm/s and yaw at 50°/s. The line shows the mean and the filled data points correspond to the neuron in panel C. In panel D significance is shown with **** for P < 0.0001 following a one-way ANOVA followed by Dunnett's multiple comparison's test done together with the data shown in Fig. S2B.

Figure 2. Interactions between optic flow and target direction

A) The data show TSDN responses to targets moving either horizontally or vertically across sideslip or lift, in the same direction as the target, or perpendicular to the target, as indicated by the pictograms. N=8. Two-way ANOVA showed P=0.2959 for target direction, P=0.7639 for optic flow direction and P=0.0002 for the interaction between target and optic flow. **B)** TSDN responses to targets moving horizontally or vertically across sideslip or lift, in

533 the opposite direction to the target, or perpendicular to the target, as indicated by the
534 pictograms. Two-way ANOVA showed P=0.0092 for target direction, P=0.0228 for optic flow
535 direction and P=0.0010 for the interaction between target and optic flow. Same N=8 in
536 panels A and B.

537 ***Figure 3. Elementary STMD input to TSDNs***

538 Responses to a leading OFF edge, trailing ON edge, or a complete black target, with a side of
539 3°, traversing a white background at 130°/s. The black data show the predicted output from
540 a motion detector that compares luminance changes from at least 2 points in space. Data
541 replotted from (34), after normalizing to its own sum. The grey data show the predicted
542 output from an elementary STMD (ESTMD), which compares luminance changes from one
543 point in space. Data replotted from (34), after normalizing to its own sum. The white data
544 show the TSDN response to the same three stimuli (N=6) after normalizing the data from
545 each neuron to its own sum.

546 ***Figure 4. The TSDN inhibition by syn-directional sideslip can be primed***

547 **A)** Raw data trace from one TSDN to a target moving across sideslip moving in the same
548 direction as the target preceding target motion, then being stationary concurrent with
549 target motion. Timing is color coded: green, preceding optic flow; red, concurrent optic
550 flow; blue, target motion. **B)** TSDN target responses are significantly inhibited by preceding
551 sideslip in the same direction as the target, compared with preceding stationary optic flow.
552 **C)** There was no significant difference between TSDN responses to targets moving across
553 syn-directional sideslip, when the sideslip moved preceding target motion compared with
554 preceding stationary optic flow (two-way ANOVA for the data in panels B and C, followed by

Post hoc Bonferroni's test: ***P=0.0004. **D)** There was no significant difference between TSDN responses to targets moving across stationary optic flow, whether this moved in the opposite direction or not preceding target motion. The grey data is the same as in panel B. **E)** There was no significant difference between TSDN responses to targets on sideslip in the opposite direction to target motion, whether the optic flow moved or not preceding target motion (two-way ANOVA for data in panels D and E, ns). Data from the same N=7 in panels B-E, with the lines showing the mean.

Figure 5. Frontal optic flow is essential

A) A pictogram of the separation of the optic flow into four distinct positions: ipsilateral (IL), dorsal (D), ventral (V) and contralateral (CL). The color coding shows the receptive field of an example TSDN, and the arrows the local motion sensitivity. **B)** TSDN responses to targets moving across syn-directional sideslip are significantly inhibited compared to stationary control (grey) if the sideslip covers the full, dorsal or ventral screen. **C)** TSDN responses to targets moving across opposite direction sideslip are significantly facilitated compared to stationary control (grey, same data as in panel B) if the sideslip covers the full, dorsal or ventral visual field. Panels B and C show data from the same neurons (N=10, one-way ANOVA followed by Dunnett's multiple comparisons test, with *P<0.05, **P<0.01).

Supplementary Information

Figure S1. The TSDN response to target motion and optic flow

A) Raw data trace from an extracellular TSDN recording. Timing of stimulus presentation indicated by colored bars (blue, target, and red, optic flow). **B)** Magnification of the raw data traces shown in panel A. **C)** Spike raster of the same neuron in response to 18 repeated trials of a target on a white background (left) or on stationary optic flow (right). **D)** To determine the TSDN response to the optic flow we first quantified each neuron's spontaneous rate, i.e. the spikes generated when viewing a white background, and used this as a threshold. For each neuron we then quantified the number of trials in which the response to the optic flow was above this threshold. This was converted to a percentage of responses. The data here show this percentage of responses across 12 TSDNs as mean ± sem. **E)** In each neuron, we quantified the mean response for those trials that were classified as responders (in panel D). This mean response was normalized to each neuron's mean response to a target traversing a white background, as throughout the rest of the paper. Data are shown as mean ± sem (N=12).

Figure S2. The TSDN response to target motion is affected by 3D optic flow

A) The response from one TSDN to a target traversing stationary optic flow (left, grey, replotted from Fig. 1C), or different types of optic flow (see red pictograms). All histograms shown as mean ± sem (n=18) at 1 ms resolution, after smoothing with a 20 ms square-wave filter. **B)** The mean response across TSDNs (N=12, same neurons as Fig. 1D) to a target traversing stationary optic flow (left, grey, replotted from Fig. 1D), or different types of optic flow. Stars indicate significance, one-way ANOVA followed by Dunnett's multiple

595 comparisons test (**P<0.01, ***P<0.001 and ****P<0.0001). Note that the one-way ANOVA
596 was done together with the data shown in Fig. 1D. Translations were simulated at 50 cm/s
597 and rotations at 50°/s. The lines show the mean and the filled data points correspond to the
598 neuron in panel A.

599 ***Figure S3. The TSDN response to vertical target motion***

600 **A)** The TSDN response to a target traversing a white background horizontally (left, grey) or
601 vertically (right, black). Histograms shown as mean ± sem (n=18) at 1 ms resolution, after
602 smoothing with a 20 ms square-wave filter. **B)** The mean spiking response of 8 TSDNs to
603 targets moving horizontally (grey, left) or vertically (black, right) over a white background.

604 ***Movie 1. TSDN response to a target over a white background***

605 The movie depicts the stimulus as displayed on the screen, with the hoverfly positioned
606 centered and perpendicular to the screen. The hoverfly was positioned ventral side up, but
607 we have rotated the movie for display purposes so the dorsal side is up. The colored lines
608 show the outline of the receptive field, mapped as described previously (23). The red data at
609 the bottom of the movie show the response of an example TSDN.

610 ***Movie 2. TSDN response to a target over a white background***

611 Same as Movie 1, but slowed down 10 times.

612 ***Movie 3. TSDN response to a target over stationary optic flow***

613 The movie depicts the stimulus as displayed on the screen, with the colored lines showing
614 the outline of the receptive field. The red data at the bottom of the movie show the

615 response of an example TSDN. In this case the optic flow was stationary, and appeared 0.5 s
616 before the target.

617 ***Movie 4. TSDN response to a target over stationary optic flow***

618 Same as Movie 3, but slowed down 10 times.

619 ***Movie 5. TSDN response to a target over syn-directional sideslip optic flow***

620 The movie depicts the response of the same example TSDN to the same target motion as in
621 previous movies, but now traversing sideslip optic flow appearing 0.5 s before the target.
622 The hoverfly was positioned at a distance of 6.5 cm. At this viewing distance, the resulting
623 optic flow simulates the type of optic flow that would be generated by the hoverfly side-
624 slipping through the world at 50 cm/s. The simulated optic flow consisted of ca 6400
625 spheres, of which roughly 1200 are projected onto the screen at any one time.

626 ***Movie 6. TSDN response to a target over syn-directional sideslip optic flow***

627 Same as Movie 5, but slowed down 10 times. Note that many of the optic flow "targets" of
628 the correct size move through the receptive field (colored contour lines).

629 ***Movie 7. TSDN response to a target over opposite direction sideslip optic flow***

630 The movie depicts the response of the same example TSDN to the same target motion as in
631 previous movies, but now traversing sideslip optic flow in the opposite direction to the
632 target.

633

634 ***Movie 8. TSDN response to a target over opposite direction sideslip optic flow***

635 Same as Movie 7, but slowed down 10 times.

636

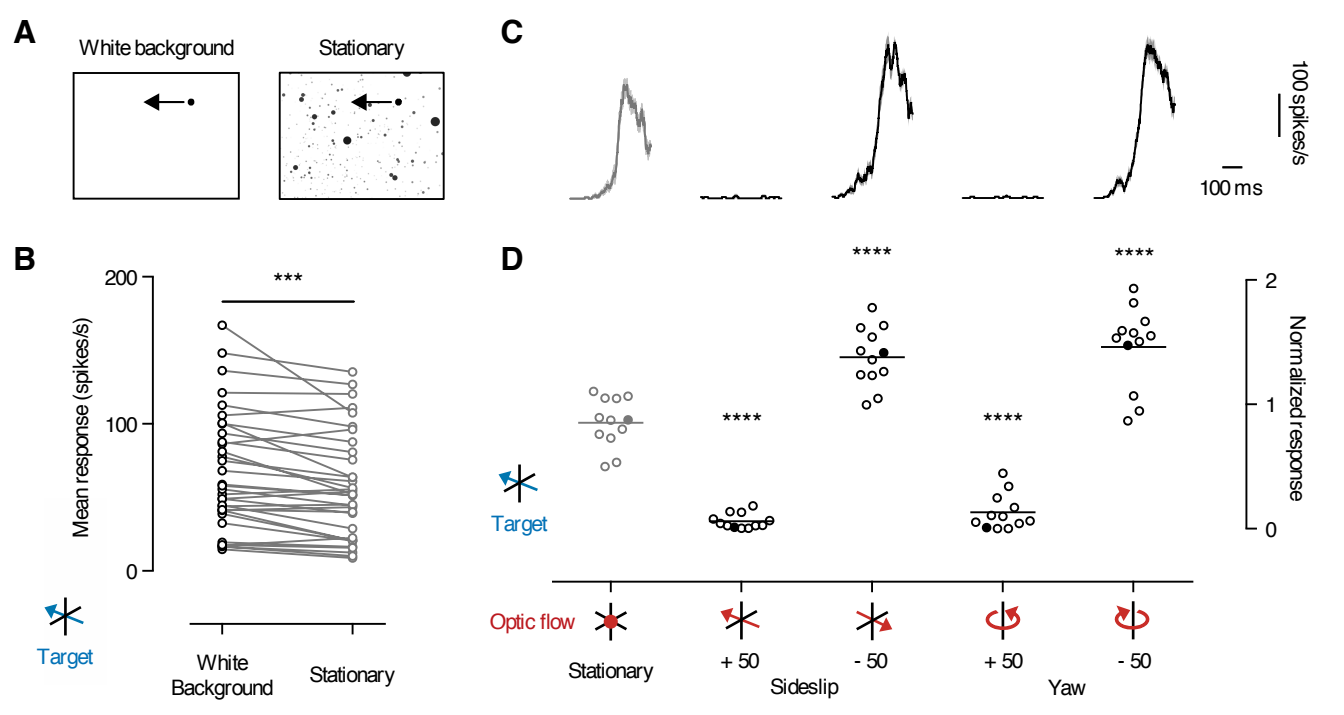
A
White background
Stationary
B
Mean response (spikes/s)
200
100
0
***
Target
White Background
Stationary
C
100 spikes/s
100 ms
D
****
****
****
****
Normalized response
2
1
0
Target
Optic flow
Stationary
+ 50
- 50
+ 50
- 50
Sideslip
Yaw

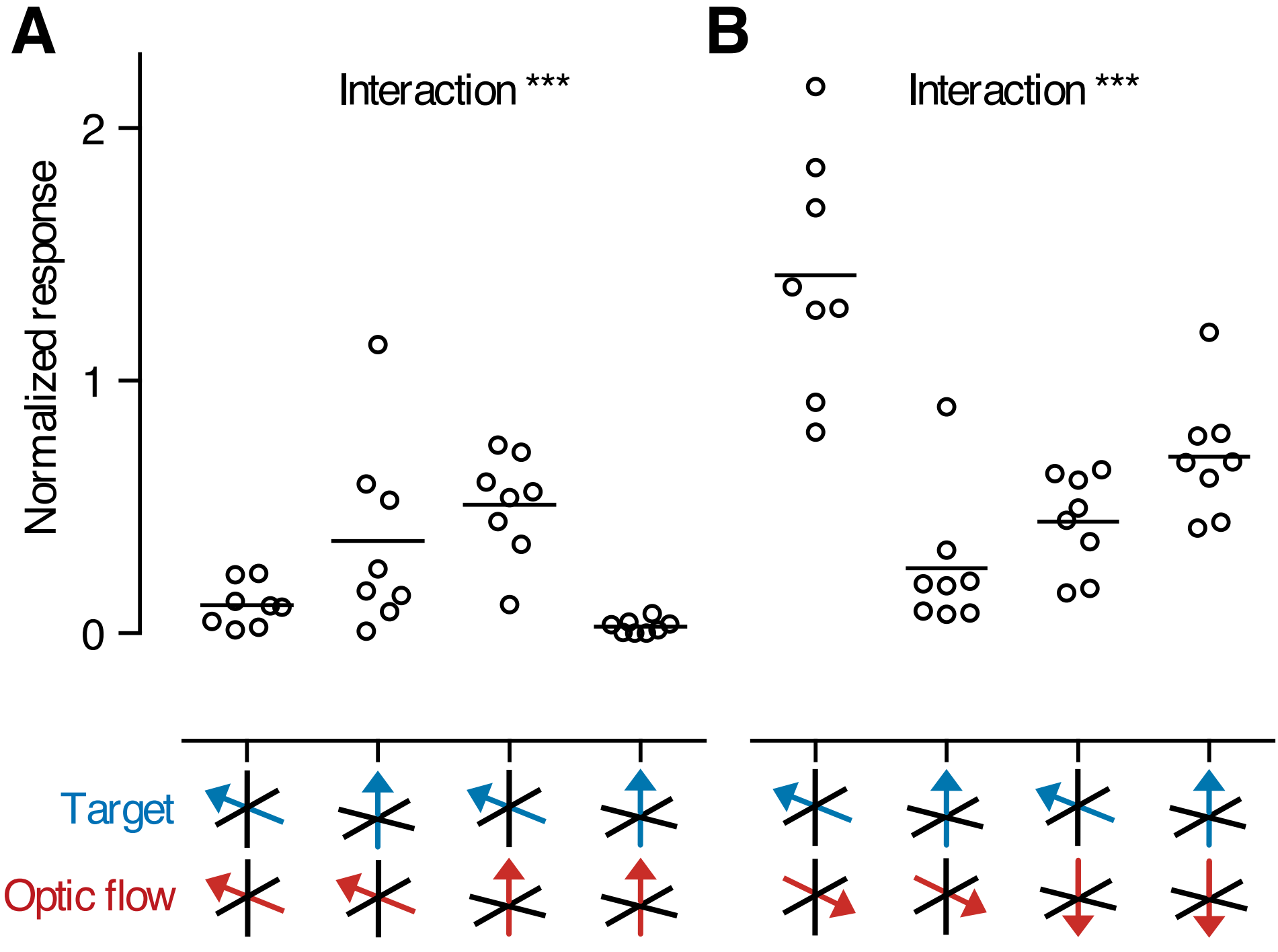
A
Interaction ***
Normalized response
2
1
0
B
Interaction ***
Target
Optic flow

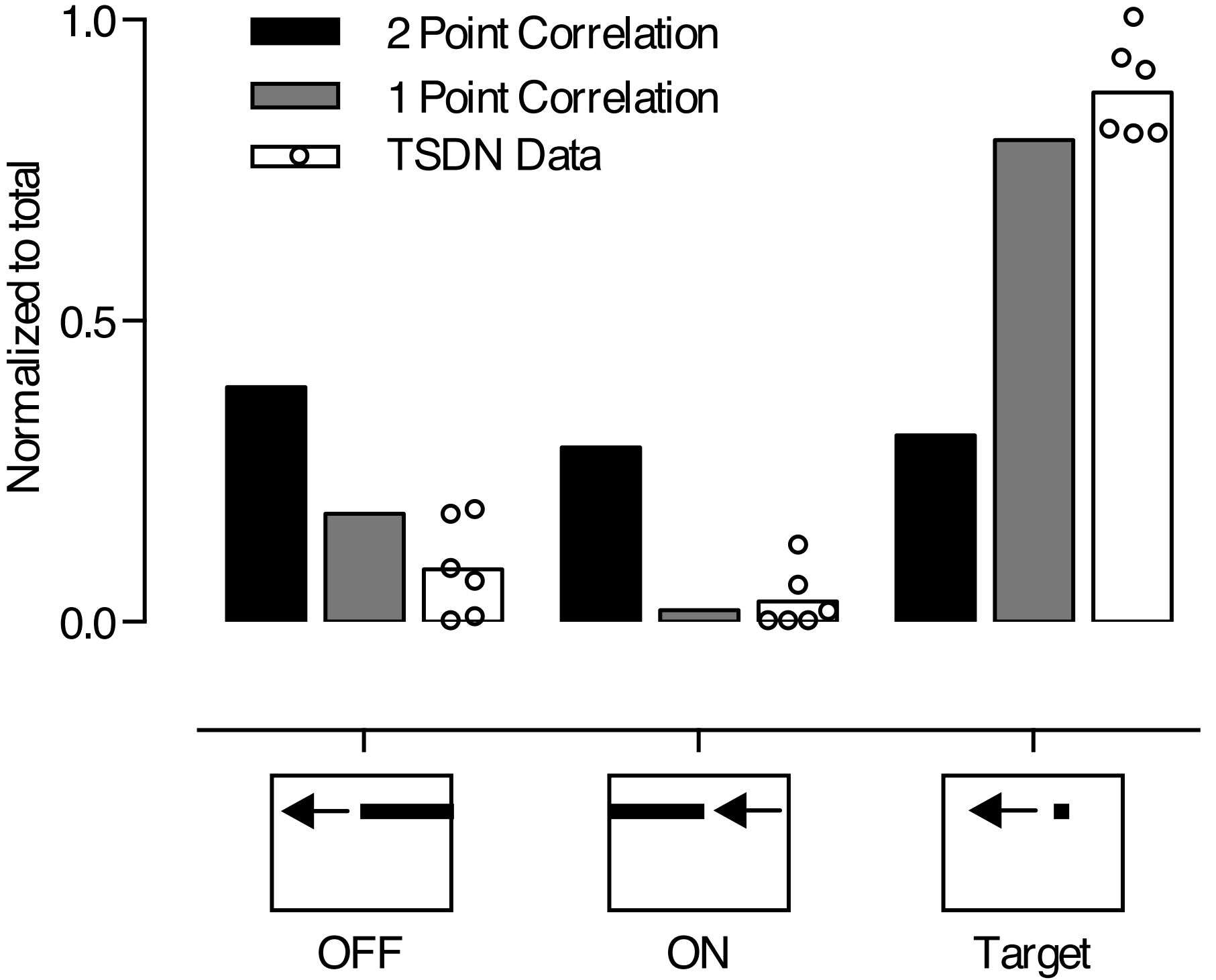
1.0
0.5
0.0
Normalized to total
2 Point Correlation
1 Point Correlation
TSDN Data
OFF
ON
Target

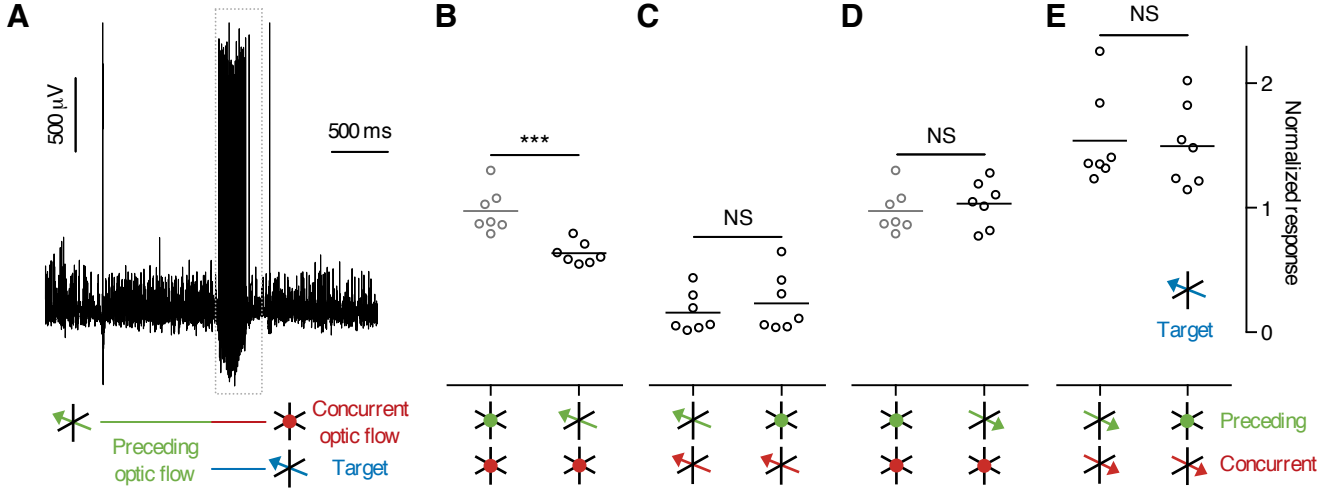
A
500 µV
500 ms
Concurrent optic flow
Preceding optic flow
Target
B
***
C
NS
D
NS
E
NS
Target
Normalized response
2
1
0
Preceding
Concurrent

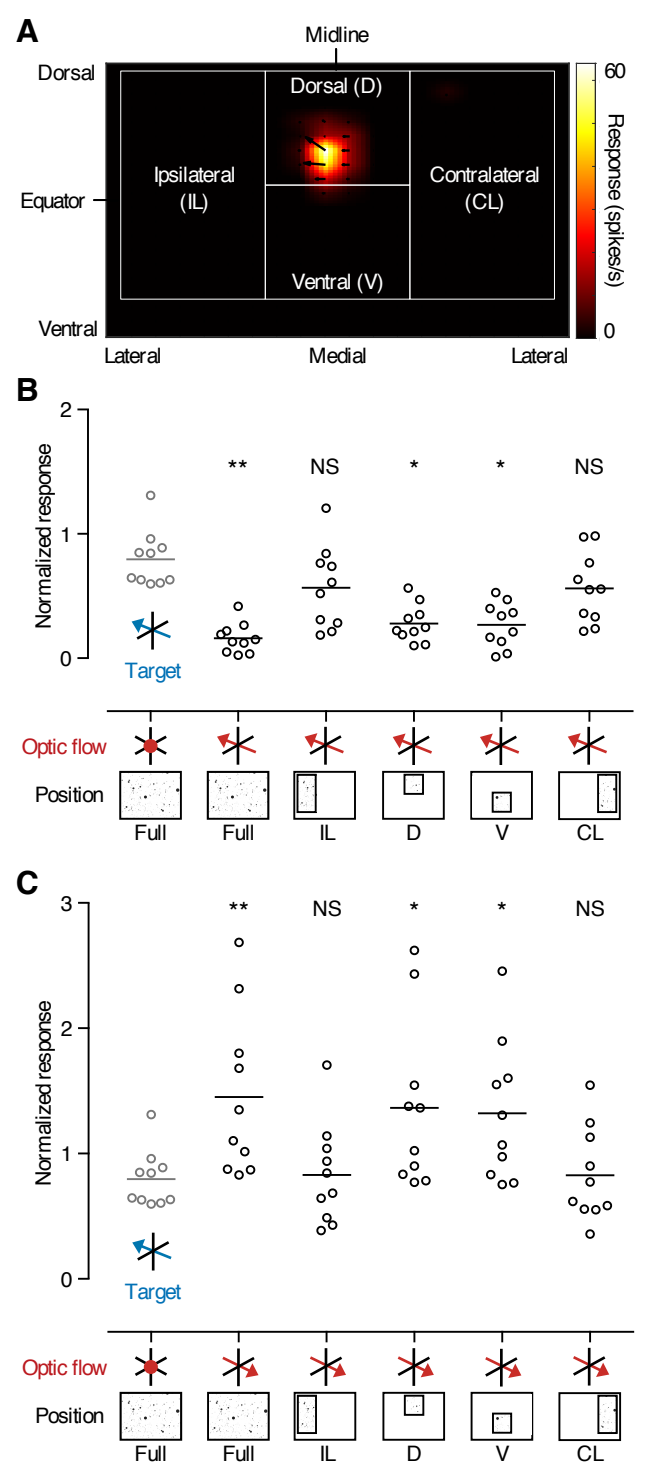
A
Midline
Dorsal
Equator
Ventral
Lateral
Medial
Lateral
Dorsal (D)
Ipsilateral (IL)
Contralateral (CL)
Ventral (V)
60
Response (spikes/s)
0
B
Normalized response
2
1
0
**
NS
*
*
NS
Target
Optic flow
Position
Full
Full
IL
D
V
CL
C
Normalized response
3
2
1
0
**
NS
*
*
NS
Target
Optic flow
Position
Full
Full
IL
D
V
CL

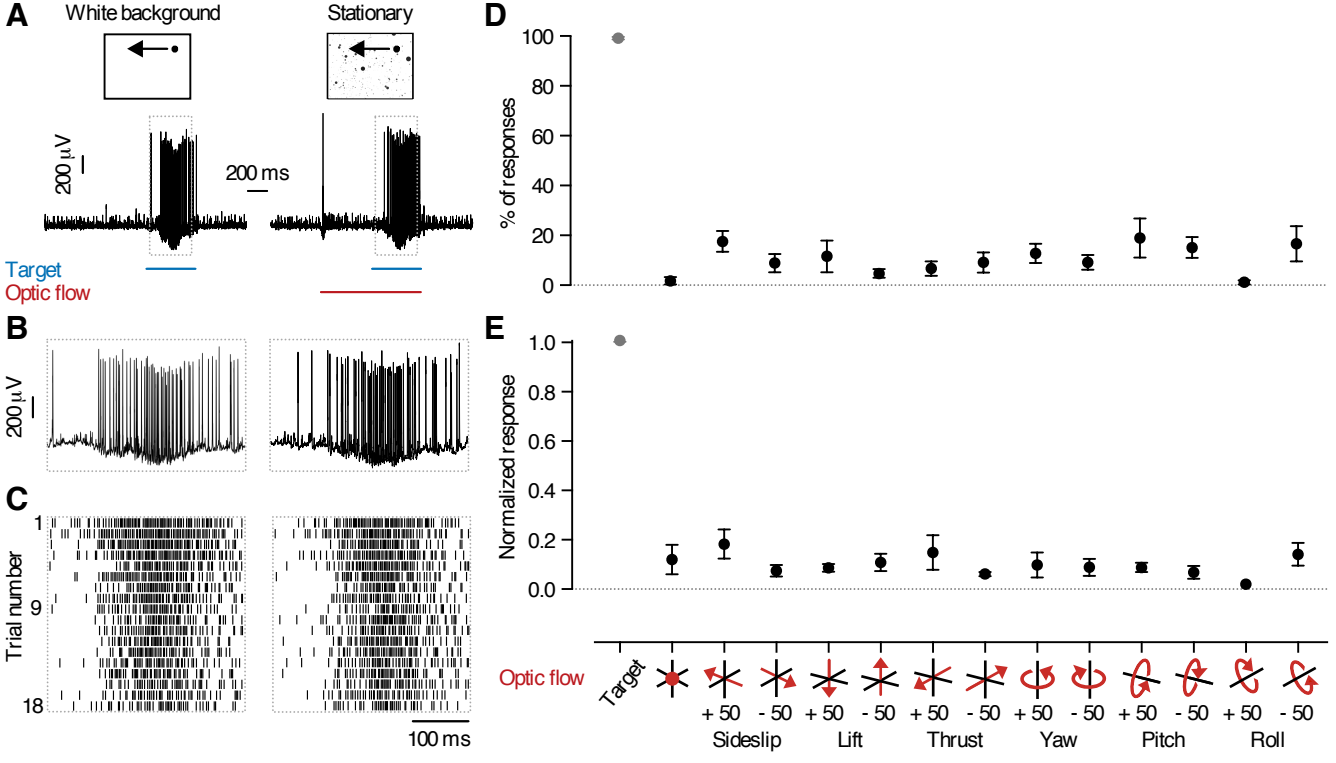
A
White background
Stationary
200 µV
200 ms
Target
Optic flow
B
200 µV
C
Trial number
1
9
18
100 ms
D
% of responses
100
80
60
40
20
0
E
Normalized response
1.0
0.8
0.6
0.4
0.2
0.0
Optic flow
Target
+ 50
- 50
Sideslip
Lift
Thrust
Yaw
Pitch
Roll

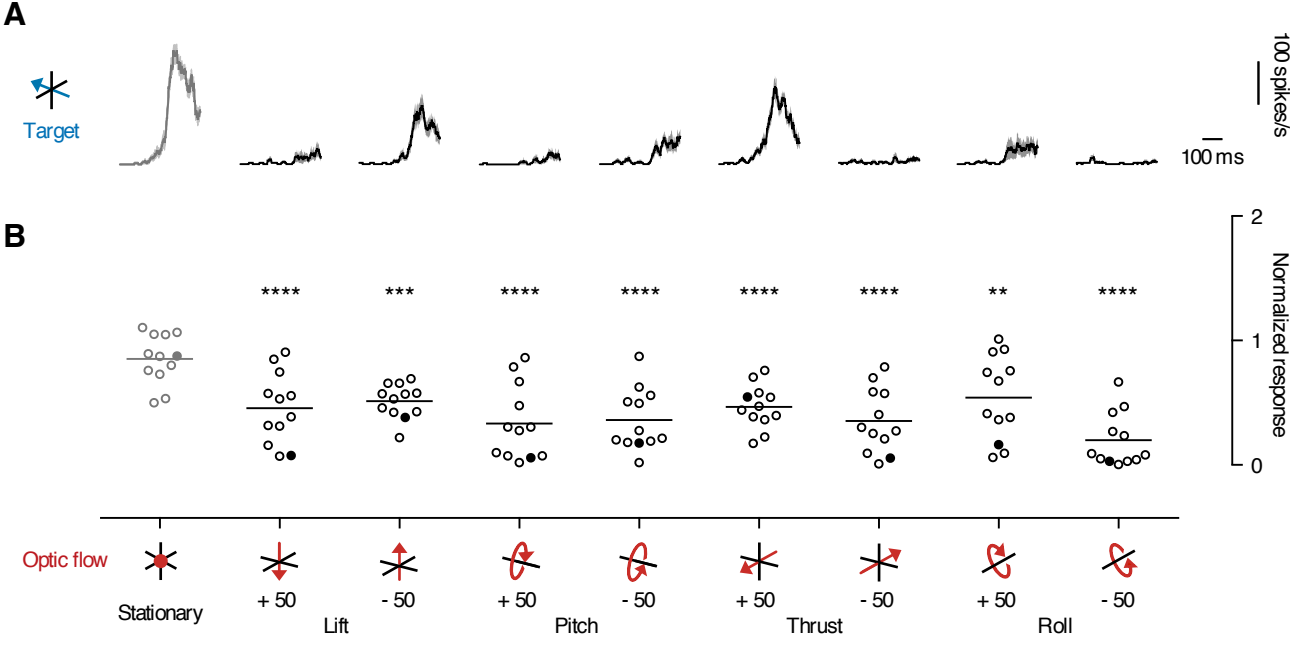
A
Target
100 spikes/s
100 ms
B
Normalized response
2
1
0
****
***
****
****
****
****
**
****
Optic flow
Stationary
+ 50
- 50
+ 50
- 50
+ 50
- 50
+ 50
- 50
Lift
Pitch
Thrust
Roll

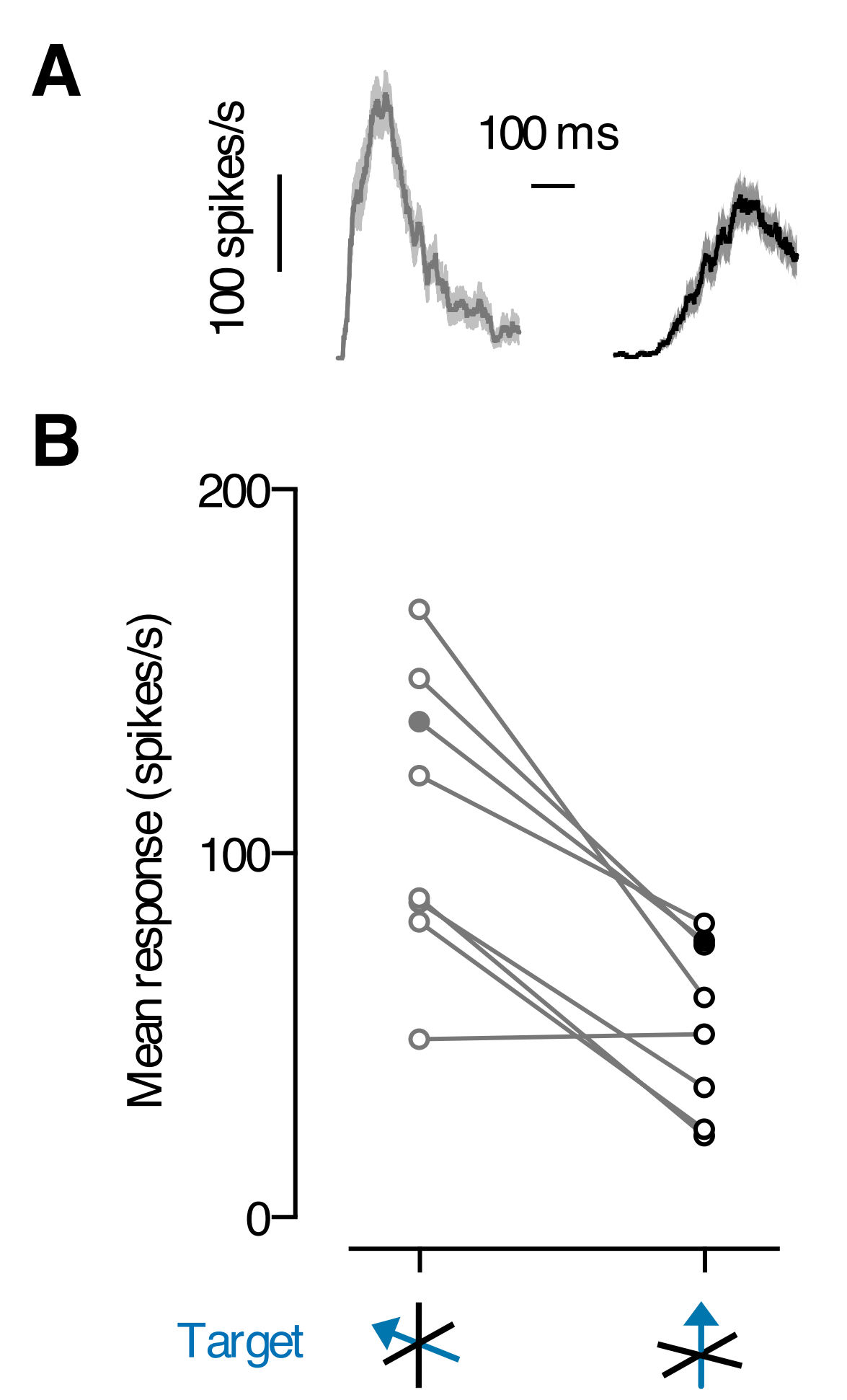
A
100 spikes/s
100 ms
B
200
100
0
Mean response (spikes/s)
Target